Fragmentation of Metal Rings by Electromagnetic Loading

Fragmentation studies on rapidly expanding metal rings are performed with electromagnetic loading. Dynamic-fracture strain and fragment-size measurements are reported for aluminum and copper

by D.E. Grady and D.A. Benson

ABSTRACT—A method is described for performing fragmentation studies on rapidly expanding metal rings. A fast-discharge capacitor system generates magnetic forces which accelerate the rings to maximum radial velocities of approximately 200 m/s corresponding to circumferential-strain rates of approximately $10^4/s$ at fragmentation. Streak-camera techniques are used to record the time-resolved motion of the rings. Fracture-strain and fragmentation experiments have been performed on samples of OFHC copper and 1100-0 aluminum.

Introduction

The fragmentation of a body due to a violent impulsive load is a complicated phenomenon which currently cannot be calculated with confidence. Dynamic loading leads to myriad interactions of stress waves which govern the fragmentation event. In addition, material-property effects and statistics of the fracture nucleation and growth process are also important.

Interpretation of dynamic-fracture experiments is complicated by the multiaxial and heterogeneous stress states occurring in most impact- or explosive-loading studies. Consequently, experimental methods which simplify the stress conditions leading to fragmentation of the body offer a better possibility of understanding the principles governing dynamic fragmentation. One attractive method is provided by radial loading of ring-shape specimens with magnetic forces in which dynamic fracture and fragmentation is brought about by the rapid application of a homogeneous one-dimensional tensile stress. The present report describes such radial-loading fragmentation experiments. Data on ring samples of 1100-0 aluminum and OFHC copper are also provided.

The expansion of rings and cylindrical shells has been used productively in the past to investigate the phenomenon of dynamic deformation. Numerous studies by direct application of explosive loading to the interior wall of cylindrical samples have been made. The method is extremely energetic, however. Experimental control is complicated by the explosive violence, product gases, and preconditioning of samples through application of the initial high-amplitude shock wave. An improved laboratory technique has been explored[1-3] where the sample ring is isolated from the explosive by a cylindrical, high-strengh metal mandrel. Recently, Warnes *et al.*[4] have extended this technique and used velocity interferometry to determine time-resolved motion of the expanding ring. Again, there is concern about shock preconditioning of the sample. Shock-wave studies indicate that material properties in metals can be severely altered by shock stresses above approximately 10 GPa.[5,6] Also, the impulse provided by this method is not sufficient to produce significant fragmentation.

The application of magnetic forces to load ring or cylindrical geometries appears to have been described in the literature first by Niordson.[7] A similar system has been described by Walling and Forrestal[8] and used by Wesenberg and Sagartz[9] to conduct fragmentation studies on large aluminum cylinders, illustrating the energy capability of this technique. Magnetic loading has several attractive features: (1) motion is imparted to the sample through continuous body forces rather than shock loading and consequently, preconditioning shock effects are eliminated; (2) loading rates are readily controlled through variation in rate and amplitude of the driving-current pulse; and (3) the method is more conducive to a laboratory environment than explosive-loading schemes. A magnetic-loading technique is not without its drawbacks, however. Since it is based on the principle of opposing forces between primary and induced currents, inductive heating, which may also have preconditioning effects, can occur in the sample material. Also, when fragmentation occurs, arcing of induced currents can result in additional local-heating effects.

The system that we have developed to conduct fragmentation experiments on metal rings is modest compared to the 250-kJ fast-discharge capacitor system described by Walling and Forrestal.[8] The present method uses approximately 10 kJ of energy and compares most closely to the work described by Niordson.[7] Implementation of the technique required additional development, however, and consequently, some description is warranted. For example, smaller experimental assemblies were found to be more sensitive to loading instabilities and different techniques were needed to apply the magnetic forces. The method

D.E. Grady and D.A. Benson are Research Scientists, Sandia National Laboratories, Albuquerque, NM 87185.

Original manuscript submitted: March 29, 1982. Final version received: July 11, 1983.

described here is suitable for uniformly expanding small metal rings to fracture at circumferential-strain rates in the vicinity of $10^4/s$. Experiments on aluminum and copper rings have been performed. An initial set of experiments was conducted at a fixed strain rate to investigate the statistical distribution in fragment sizes. In a subsequent set of tests, the strain-rate dependence of fragmentation and fracture strain was explored.

Experimental Method

Radial motion is imparted to a ring-shaped sample by forces between opposing currents as illustrated in Fig. 1. Current of magnitude i_1 is discharged from a capacitor system into one or more current turns. An oppositely directed current of magnitude i_2 is induced in the metal ring. The ring is accelerated radially by a force which is proportional to the product of the two currents, i_1 and i_2, while the opposing force on the primary turns is supported by a rigid mandrel.

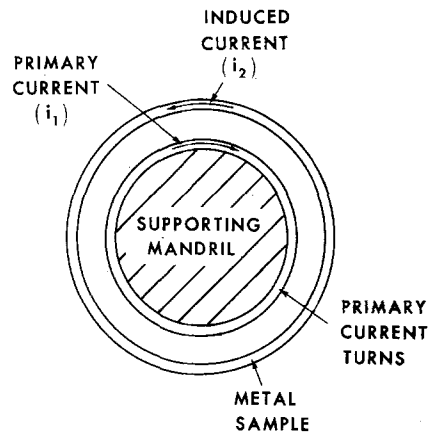

Fig. 1—Geometry of pulsed-current magnetic-expanding-ring technique

Electrical System

The pulsed-power system used to electromagnetically accelerate the ring sample is a fast-discharge capacitive-storage device. Four high-energy density capacitors of 100 μf, each charged to voltages between 2 and 3 kV, are used for the present work. Each capacitor is independently discharged through primary turns using grounded-grid hydrogen thyratrons as switches. A high-power, 0.5-ohm ballast resistor is provided on the system output to protect against open-circuit load conditions. The transmission line from the pulsed-power system consists of parallel 2/0 copper-cable conductors approximately two meters in length. While this line minimizes resistive losses, the substantial cable inductance limits the pulse-current rise time. Figure 2 shows the four-section pulsed-power system with details of the high-voltage circuitry for one of these sections. Switches depicted in section one are relays for the control of charge, dump and trigger functions of the pulser system.

In the present tests, the four thyratron circuits are discharged simultaneously and produce a total current of 20-kA amplitude in a 100 μs full-width duration pulse. The current rate on the leading edge of this pulse is $\sim 5x\ 10^8\ A/s$. The current in the primary coil of the sample is measured with a 0.005-ohm coaxial-current-viewing resistor (CVR) placed on the discharged circuit. The CVR voltage is monitored by a differential amplifier to determine the current-pulse characteristics.

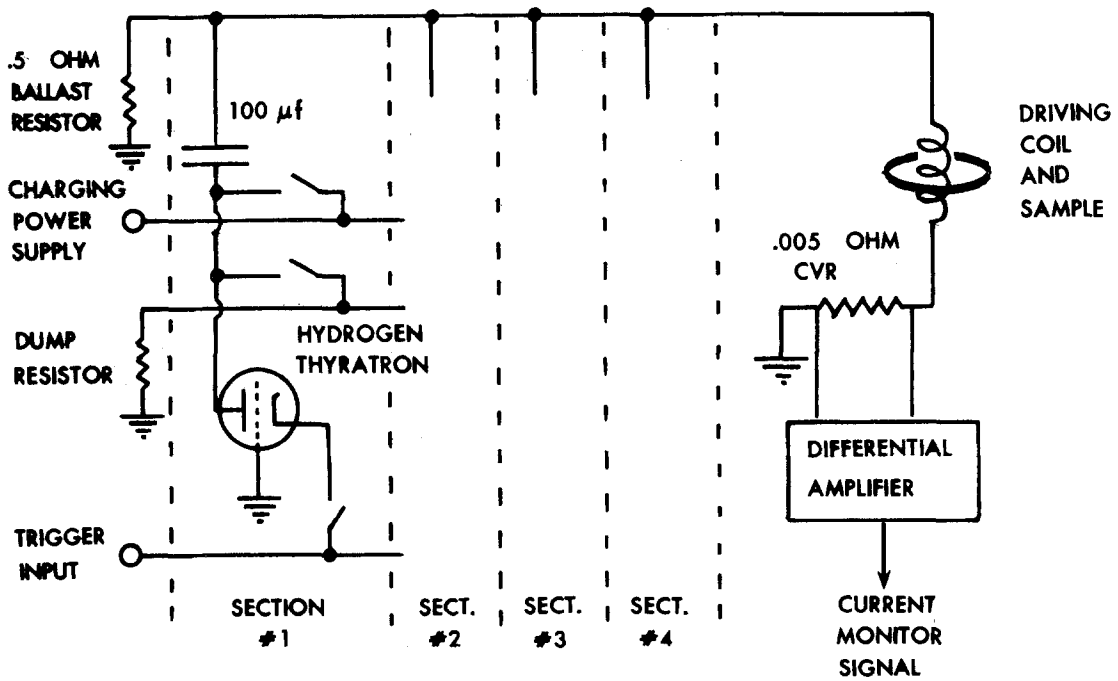

Fig. 2—Diagram of pulsed-power system used to electromagnetically accelerate metal rings

Loading System

Initial calculations indicate that the electrical system had sufficient energy to impart radial velocities approaching 500 m/s to reasonable-size ring samples. The most effective (and stable) geometry for coupling the magnetic forces was not immediately clear, however. Initially, a cylindrical copper-current sheet, similar to the method of Walling and Forrestal,[8] approximately 30 mm in diameter and 10 mm in height, was used for the primary. It was found that the copper foil would collapse and the ring tended to move longitudinally as well as radially. In addition, the single-current sheet provided insufficient forces to achieve the desired velocities. Several iterations led to a solenoid design for the primary. Two- to eight-turn solenoids were tried; six turns over a length of one centimeter were found to be about optimum. Initially, we attempted a complicated crossover pattern while winding the primary to avoid the helicity inherent in a solenoid. Later, in using a solenoid geometry, the slight perturbation in radial motion due to helicity was investigated and found to be acceptable. The final design resulted in a six-turn AWG No. 18 copper-wire primary wound on a 14-turns-per-inch threaded Plexiglas mandrel. A thin (.002-in.) Plexiglas cylinder insulated the primary coils from the sample ring. The thickness of this cylinder was found to be an important feature in governing the coupling efficiency of the primary current to the sample ring. An exploded view of the loading assembly including a sample ring is shown in Fig. 3.

With this system, uniform radial loading of metal rings to velocities of approximately 200 m/s at fragmentation was achieved. The rings were fragmented into as many as thirteen pieces depending on material and loading conditions. The high-velocity fragments were arrested and soft recovered in a liner of mixed beeswax and vaseline.

During initial development of the method various ring diameters and cross-section geometries were tried. Ultimately, sample dimensions of 32-mm diam and 1-mm^2 cross section were used. This geometry was compatible with the current available from the fast-discharge capacitor system and was large enough to conduct useful fragmentation experiments. Initial experiments were conducted on rings of OFHC copper and 1100-0 aluminum. Specimens were machined from 50-mm diam bar stock.

Time-resolved Motion Measurements

Motion of the expanding rings was monitored photographically. Initially, an open-shutter camera technique was used with the camera focused on the plane of expansion of the ring. Exposure was controlled by back lighting the desired image with a Xenon flash lamp. The minimum-length light pulse available had a duration of 50 μs and

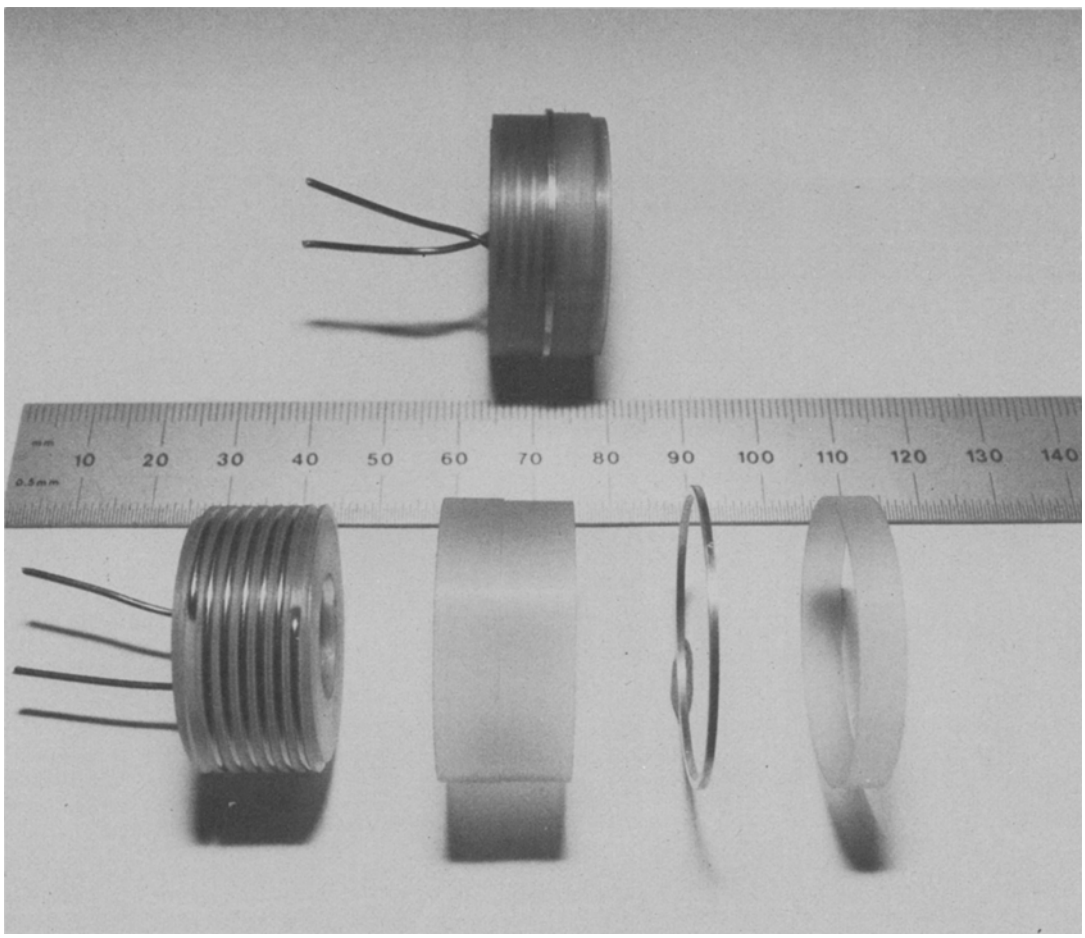

Fig. 3—Components of electromagnetic-expanding-ring system

could be delayed to any desired time in the ring-expansion event. Because of the relatively long-duration flash exposure, the photographic record of the ring in flight was spatially blurred. Although not useful for quantitative measurements, the photographs verified that the expansion process was radially uniform and stable.

Quantitative displacement-time records with improved time resolution were obtained with a streak-camera technique. In this case, the image of the ring-expansion plane was projected on the slit of the streak-camera system using a 305-mm focal length $f/4.5$ lens, giving an effective magnification of the ring image at the streak-camera slit of 1.60. The slit consisted of a photo-etched bronze foil with a slit width of 0.3 mm and length of 12.7 mm. Crossing the slit at 1.0-mm intervals were narrow bridges which provided a spatial calibration for the photographic records. Light passing through the slit was optically focused on the photocathode of an image-converter tube producing the actual streak image. The image was then recorded on film with a streak-camera scale of 100 μs.

Figure 4 shows the streak photograph of one test. The capacitor-bank discharge was initiated 20 μs after the start of the streak. Acceleration of the ring was evident shortly after this time as the ring lifted clear of the mandrel. After a displacement of ~1 mm, the magnitude of acceleration was reduced to a nearly constant-velocity condition in the remainder of the record. The field of view in Fig. 4 corresponds to a specimen strain of approximately 40 percent. A larger field of view was required in the copper-ring tests.

Resistive Heating

As the current in the primary coil rises, it induces a current in the test sample. These opposing currents result in the force which electromagnetically accelerates the sample ring to fragmentation. A second feature of the induced current is that it resistively heats the ring, and may in some cases produce sufficient temperature increases to modify the sample properties. The heating depends on the local resistivity of the deforming ring, a quantity which is not easily determined. Also, we have not measured the current in the ring and can only infer it from the calculated driving force. With these limitations

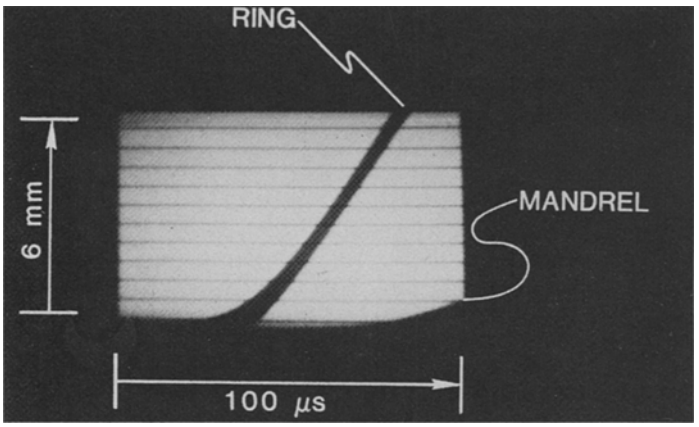

Fig. 4—Strak-photograph image of expanding-ring experiment on aluminum

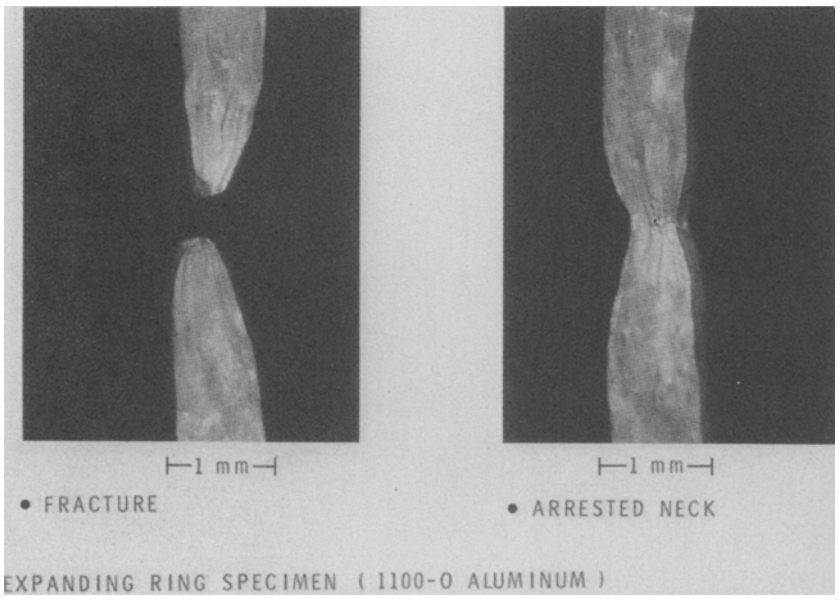

Fig. 5—Photograph of fracture and arrested-neck region from dynamic expansion of an aluminum ring

in mind, the induced temperature rise of the ring has been estimated as shown below.

For the six-turn primary coil used in these tests a constant-current rate of $5x\ 10^8\ A/s$ was measured during the pulse rise time. We estimate from measured ring velocities, a current-coupling efficiency of 0.1 for the primary/secondary coil configuration and predict a current rate of $3.0x\ 10^8\ A/s$ in the sample ring.

For a ring with cross-sectional area A, resistivity σ, density ϱ, and heat capacity C_p, the temperature increase as a function of time $T(t)$, due to a current rate $\dot{I}$, will be

$$T(t) = \frac{\sigma}{3\varrho C_p A^2}\dot{I}^2 t^3 .$$

Such a ring will continue to accelerate and heat until it becomes electrically decoupled from the primary coil. In the case of Fig. 4, this requires about 35 μs. With this time and parameters for 1.0-mm² area ring, temperature increases of 8 °K for copper and 15 °K for aluminum are estimated. Thus, resistive heating of this order can be anticipated during the expansion process.

Fragmentation Experiments

The results of twelve fragmentation tests on both 1100-0 aluminum and OFHC copper metal rings are provided in Table 1. All tests were conducted at a fixed-capacitor voltage of 3 kV. In addition to time-resolved strain and strain-rate measurements, fragments were recovered and the number and distribution in sizes were determined. The number of arrested necks occurring in each test was also determined.

Strain-rate Measurement

The radial motion determined from the streak-camera records showed an initial-acceleration region followed by an interval of nearly constant velocity. Fracture of the ring occurred within this interval. The velocities for copper specimens were somewhat lower than for aluminum, consistent with the mass difference. Reproducibility of the loading system is best illustrated by the velocity data in Table 1. There is approximately a 20-percent maximum variation in velocity for the same material. Strain rates reported in Table 1 are the velocity divided by the initial-ring radius.

Fracture Strain

During the initial expansion, work hardening dominates the plastic flow and deformation produces a stable increase in the ring diameter and a corresponding reduction in the cross-sectional area. As area reduction overcomes strain or strain-rate hardening, the deformation process becomes unstable leading to the nucleation of necks and ultimately fragmentation of the ring. This instability can, in principle, be predicted through criteria derived to predict the onset of necking.[10] These derivations were not focused on the high-tensile loading-rate regime, however. Consequently, they do not account for effects of material inertia. Recent work by Rajandran and Fyfe[11] and Johnson[12] do account for inertia, as well as important material properties, and represent significant advances in understanding the dynamic-fracture phenomena.

Strain at fracture is reported in Table 1 for the present experiments. Strain is determined by post-test measurement of fragment elongation and is discussed further in the next section. The 1100-0 aluminum specimens achieve a fracture strain of approximately 42 percent. OFHC copper is appreciably more ductile, reaching fracture strains of about 62 percent.

Fracture Mode

Fracture in both aluminum and copper occurs through the nucleation and ductile growth of a distribution of necking regions as the deformation process becomes unstable. This would contrast with brittle materials in which fragmentation by shear- or extension-fracture would occur. In Fig. 5, a photograph of a completed fracture and an arrested neck is shown. Fragmentation initiates through the growth of the neck and is completed by extension fracture through the hardened material within the neck region. The arrested neck results from the arrival of a relieving stress wave from a nearby fracture which removes the driving force before fracture is completed. The number of arrested necks observed in each test is listed in Table 1.

TABLE 1—FRAGMENTATION EXPERIMENTS

Test No.	Material*	Ring Velocity (m/s)	Strain Rate V/r μs^{-1}	Number of Fragments	Number of Arrested Necks	Strain at Fracture r/r_0^{-1}
1	Al	190	.012	13	17	0.44
2	Al	192	.012	13	11	0.42
3	Al	208	.013	11	13	0.40
4	Al	217	.014	13	13	0.45
5	Al	182	.011	11	14	0.43
6	Al	220	.014	11	20	0.45
7	Cu	140	.009	10	11	0.66
8	Cu	**	**	9	15	0.65
9	Cu	134	.009	9	15	0.61
10	Cu	138	.009	11	9	0.61
11	Cu	**	**	11	13	0.61
12	Cu	132	.010	11	12	0.60

*Material is 1100-0 aluminum and OFHC copper.

**Velocity measurements were not obtained on these tests although they were performed at the same capacitor voltage.

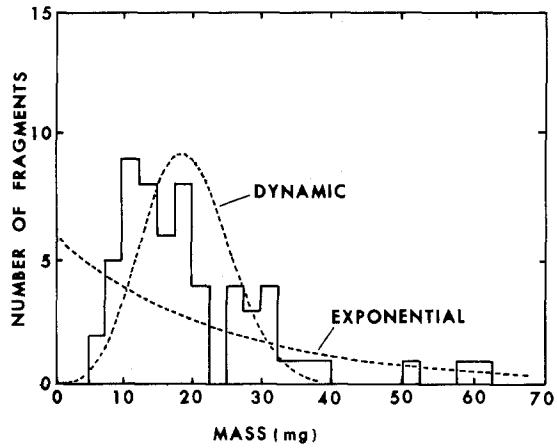

Fig. 6—Distribution in mass of fragments obtained from expanding-ring tests on 1100-0 aluminum

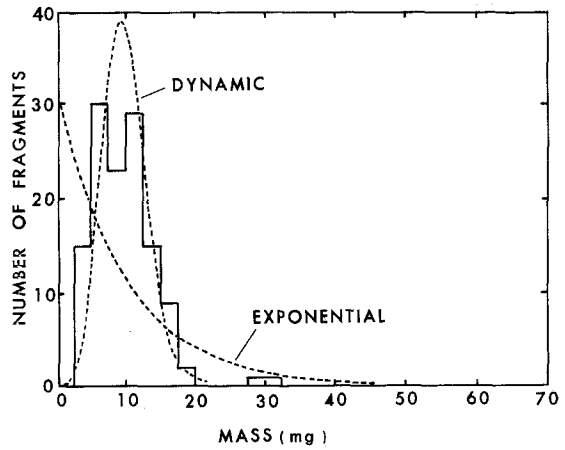

Fig. 7—Distribution in mass of fragments obtained from expanding-ring tests on OFHC copper

Statistics of Fracture

All tests in the present series were performed under similar loading conditions. With the exception of the slight difference between copper and aluminum samples, strain rates were nominally the same. Fragments from all tests were collated, counted and each was weighed separately. From this a statistical-size distribution for both copper and aluminum was determined.

In Fig. 6, the distribution in size (actually fragment mass) of the fragments resulting from the six experiments on 1100-0 aluminum is shown. Similar data for copper are shown in Fig. 7. The data are not sufficient to undertake a detailed comparison with existing statistical-fragmentation theories; however, some modest considerations are worthwhile. An appreciable portion of current fragmentation theory finds its roots in ideas introduced by Mott in the 1940's.[13,14] Some of his relations are still applied directly and some confusion in their application remains. In his early work,[13] Mott suggested that the distribution of fragment size in a one-dimensional problem might be determined strictly by the Poisson distribution of random breaks in a length of line. This approach leads to an exponential distribution in fragment size:

$$\frac{dN}{dX} = \frac{N_0}{\sigma} e^{-\frac{X}{\sigma}} \tag{1}$$

where N_0 is the total number of fragments, X is the size and σ is the scale parameter of the distribution. The two-dimensional extrapolation of this relation provided the extensively used Mott expression relating the number of fragments to the exponential square root of the fragment mass.[13]

In later work, Mott recognized the importance of time-related effects in determining dynamic-fragment distributions.[14] The occurrence of fracture at a point on the line would cause a propagating release of tensile stress in regions near the fracture and change the sample space in which further fracturing could occur. Under specific assumptions of dynamic-tensile fracture in a one-dimensional plastic body, the ideas of Mott have been recently incorporated in a statistical-fragmentation framework.[15] The resulting distribution function derived in that work is

$$\frac{dN}{dX} = \frac{N_0}{\sigma} \frac{\beta^2}{4} e^{-\frac{1}{4}\left(\frac{X}{\sigma}\right)^3} \int_0^X \left[\left(\frac{X}{\sigma}\right)^2 - \xi^2\right] e^{-\frac{3}{4}\frac{X}{\sigma}\xi^2} d\xi \tag{2}$$

where β is a number near unity and again σ is the distribution-scale parameter. Both distribution functions are compared with the fragment-size data in Figs. 6 and 7. The exponential distribution clearly does not describe the dynamic data. Equation (2) is certainly better, but there is a significant number of large fragments well outside of the predicted range and the lack of fragments in certain size ranges is disturbing.

Equation (2) was derived based on the assumption of instantaneous fracture at each point where a break occurs. As suggested by the photograph in Fig. 5, fracture occurs by the nucleation and growth of a neck in the body and significant stress unloading can occur in the vicinity of a neck before actual separation. Consequently, the actual situation appears to be more complicated than the simplifying assumptions suggested by Mott.[14]

Strain-rate Experiments

A second series of experiments was performed on 1100-0 aluminum and OFHC copper where the initial capacitor voltage was selected to vary the strain rate at the point of fracture. Velocities ranging from about 20 to 200 m/s were achieved corresponding to strain rate from about $10^3/s$ to $10^4/s$. At the lowest voltages, it was not uncommon to recover an expanded but unfractured ring. These were not included in the present set of data. In these experiments, the number of fragments and the fracture strain were determined and correlated with fracture velocity. Static-tensile pull tests were performed on dog-bone specimens of the same materials to compare dynamic and static strain. The results of the dynamic experiments are included in Table 2.

Fragment Number

In this series of tests, 1 to 12 fragments were recovered, depending on the velocity achieved in the experiment. The fragment numbers are plotted against the velocity in Fig. 8. The data illustrate the expected dependence of fragment size on strain rate, showing an approximately linear behavior over the range achieved. Both the number of fragments and trend of the data are

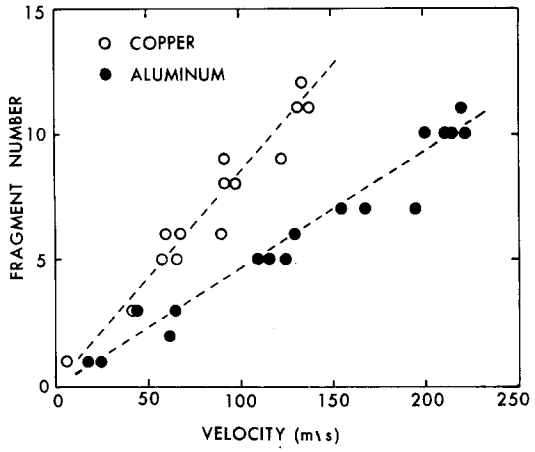

Fig. 8—Dependence of the number of fragments on the velocity of fragmentation. Strain rate is proportional to the velocity

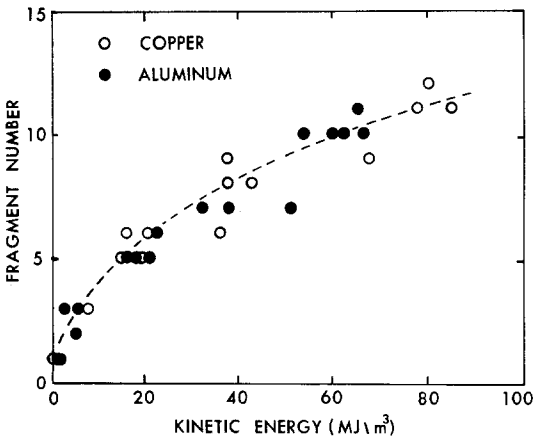

Fig. 9—Fragment-number dependence on kinetic energy

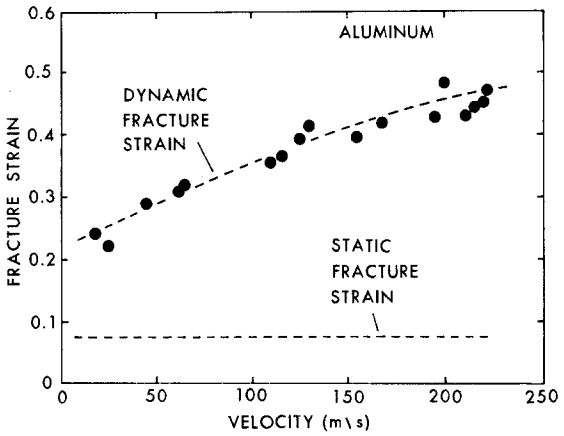

Fig. 10—Dynamic- and static-fracture strain in aluminum

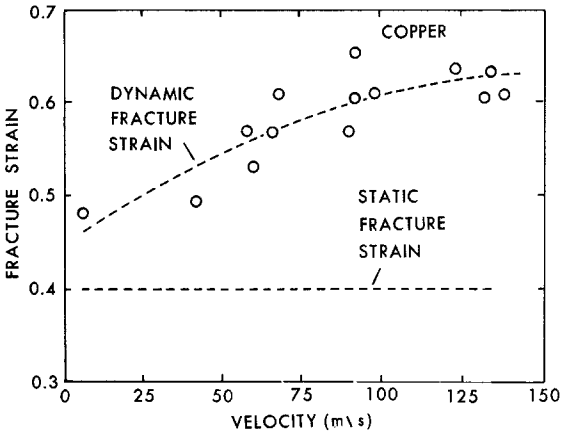

Fig. 11—Dynamic- and static-fracture strain in copper

in line with the strain-rate-dependent fragmentation calculation of Ref. 16, although the functional behavior seems to indicate a dependence on the ring geometry.

In Fig. 9, the fragment-number data are replotted as a function of the kinetic energy, $\frac{1}{2}\rho u^2$, where ρ is either the density of aluminum or copper. The data correlate well with kinetic energy as suggested by dimensional considerations.

Fracture Strain

Without an extensive discourse on the subject, it should be recognized that the definition of a dynamic fracture strain is somewhat nebulous. Strain at the point of initiation of unstable neck growth would be an overly conservative measure, in that growth of the neck to fracture completion occurs over an appreciable time. We have estimated times on the order of 10 μs. Beyond the point of instability, however, strain is nonuniformly distributed about the circumference due to a distribution of growing necks and some average-strain measure must be considered. As an experimental measure of the fracture strain, we have chosen the unambiguous method of measuring the total length of the collected fragments and comparing with the initial ring circumference. This measure of strain differs from that of Rajandra and Fyfe[11] who attempted to determine a failure strain corresponding to the onset of fracture. The fracture strain in the present study is more in line with that used by Winter[17] and Stelly *et al.*[18] The dynamic-fracture strain data for aluminum and copper are provided in Table 2 and plotted in Figs. 10 and 11.

To assess the importance of dynamic-loading effects on the fracture strain, static experiments were performed on small dog-bone specimens. Specimens were machined to the same cross-sectional area out of the same bar stock used for the rings. The same orientation with respect to material fabric was also achieved. Samples were pulled in tension at a constant strain rate of $3x10^{-4}/s$.

Tests on aluminum showed a rapid work hardening to a flow force of approximately 110 N. From a total of six tests, a nominal fracture strain of 0.075 was established. The copper specimens work hardened somewhat slower to approximately 205 N. From four tests, a static-fracture strain of 0.40 was determined.

Comparison of the dynamic- and static-fracture strain is made for aluminum and copper in Figs. 10 and 11, respectively. For aluminum the dynamic-fracture strain is significantly larger and increases with the velocity or, equivalently, the strain rate at fracture. The behavior of copper is similar but less pronounced. The differences in static- and dynamic-fracture strain compare in trend with the observations of Rajandran and Fyfe[11] and the strain-rate dependence agrees with the work of Winter.[17]

TABLE 2—STRAIN-RATE EXPERIMENTS

Test No. and Material	Fragment Number	Ring Velocity (m/s)	Fracture Strain	Test No. and Material	Fragment Number	Ring Velocity (m/s)	Fracture Strain
1 (Al)	1	18	.241	17 (Al)	10	222	.470
2 (Al)	1	25	.222	18 (Cu)	1	6	.481
3 (Al)	3	45	.288	19 (Cu)	3	42	.493
4 (Al)	2	62	.307	20 (Cu)	5	58	.567
5 (Al)	3	65	.318	21 (Cu)	6	60	.530
6 (Al)	5	110	.353	22 (Cu)	5	66	.566
7 (Al)	5	116	.363	23 (Cu)	6	68	.607
8 (Al)	5	125	.391	24 (Cu)	6	90	.567
9 (Al)	6	130	.411	25 (Cu)	8	92	.652
10 (Al)	7	155	.393	26 (Cu)	9	92	.603
11 (Al)	7	168	.416	27 (Cu)	8	98	.608
12 (Al)	7	195	.425	28 (Cu)	9	123	.635
13 (Al)	10	200	.481	29 (Cu)	11	132	.603
14 (Al)	10	211	.427	30 (Cu)	12	134	.631
15 (Al)	10	215	.441	31 (Cu)	11	138	.607
16 (Al)	11	220	.450				

Summary

An experimental method has been described which was developed to conduct dynamic-fracture and fragmentation experiments under conditions approximating uniform one-dimensional tensile loading. The objective was to develop an economical and rapid technique whereby sufficient tests can be conducted to explore the energetics and statistics of fragmentation under controlled-loading conditions. Magnetic methods are an extremely attractive technique for accomplishing these goals, with inductive heating being the one possible drawback.

Strain rates to about $10^4/s$ are currently being achieved and measured by streak-camera methods. A strain-rate range of about $10^3/s$-$10^5/s$ appears achievable with this experimental technique.

Experimental results in the initial set of tests focused on the characteristics of fragmentation in ductile metals at a fixed strain rate. Strains due to fracture are large due to the initial dead, soft condition of the metal. Fracture is through the nucleation and growth of necking regions. Failure occurs through multiple fragmentation with a characteristic distribution in fragment size.

We have compared the fragmentation data with both the initial and later concepts of fragmentation statistics put forth by Mott.[9,10] The comparison clearly illustrates the better applicability of the later ideas. The assumption of instantaneous fracture does not appear to be appropriate to the present fragmentation data, however, since arrested necks are observed which play a role in the tensile unloading process but are not accounted for in the fragment statistics.

In the subsequent set of experiments, the strain rate at fracture was varied. The results demonstrated that the number of fragments is a sensitive function of the strain rate. Measurements of dynamic-fracture strain were also found to depend on strain rate.

Acknowledgment

This work, performed at Sandia National Laboratories, was supported by the U.S. Department of Energy under contract-number DE-AC04-76DP00789.

References

1. Johnson, P.C., Stein, B.A. and Davis, R.S., "Measurement of Dynamic Plastic Flow Properties under Uniform Stress, in Symposium on the Dynamic Behavior of Materials," ASTM Special Publications No. 336, 195 (1963).

2. Perrone, N., "On the Use of the Ring Test for Determining Rate-sensitive Material Constants," EXPERIMENTAL MECHANICS, **8** *(5), 232-236 (May 1968).*

3. Hoggatt, C.R. and Recht, R.F., "Stress-Strain Data Obtained at High Rates Using an Expanding Ring," EXPERIMENTAL MECHANICS, **9** *(10), 441-448 (Oct. 1969).*

4. Warnes, R.H., Duffey, T.A., Karpp, R.R. and Carden, A.E., "An Improved Technique for Determining Dynamic Material Properties Using the Expanding Ring, in Shock Waves and High-Strain-Rate Phenomena in Metals," ed. M.A. Meyers and L.E. Murr, Plenum Press, New York, 23 (1981).

5. Asay, J.R. and Chhabildas, L.C., "Determination of the Shear Strength of Shock-Compressed 6061-T6 Aluminum in Shock Waves and High-Strain-Rate Phenomena in Metals," ed. M.A. Meyers and L.E. Murr, Plenum Press, New York, 47 (1981).

6. Grady, D.E., Asay, J.R., Rohde, R.D. and Wise, J.L., "Microstructure and Mechanical Properties of Precipitation Hardened Aluminum under High Rate Loading," Proc. 29th Sagamore Army Mat. Research Conf., Lake Placid, NY, July 19-23, 1982, (in press).

7. Niordson, F.I., "A Unit for Testing Materials at High Strain Rates," EXPERIMENTAL MECHANICS, **5** *(1), 29-32 (Jan. 1965).*

8. Walling, H.C. and Forrestal, M.J., "Elastic-Plastic Expansion of 6061-T6 Aluminum Rings," J. AIAA, **11** *(8), 1196 (1973).*

9. Wesenberg, D.L. and Sagartz, M.J., "Dynamic Fracture of 6061-T6 Aluminum Cylinders," J. Appl. Mech., **44**, *643 (1977).*

10. Argon, A.S., "Stability of Plastic Deformation, in The Homogeneity of Plastic Deformation," Amer. Soc. Metals, Metals Park, OH, 161 (1973).

11. Rajandran, A.M. and Fyfe, I.M., "Inertia Effects on the Ductile Failure of Thin Rings," J. Appl. Mech., **49**, *31 (1982).*

12. Johnson, J.N., "Ductile Fracture of Rapidly Expanding Rings," J. Appl. Mech. (in press).

13. Mott, N.F., "Fragmentation of HE Shells: A Theoretical Formula for the Distribution of Weights of Fragments," AORG Memorandum 24 (1943).

14. Mott, N.F., "Fragmentation of Shell Cases," Proc. Roy. Soc. London, **300**, *300-308 (1947).*

15. Grady, D.E., "Fragmentation of Solids under Impulse Stress Loading," J. Geophys. Res., **86**, *(B2), 1047 (1981).*

16. Grady, D.E., "Local Inertial Effects on Dynamic Fragmentation," J. Appl. Phys., **53**, *322 (1982).*

17. Winter, R.E., "Measurement of Fracture Strain at High Strain Rates," Inst. Phys. Conf. Ser. (47), 81 (1979).

18. Stelly, M., Legrand, J. and Dormeval, R., "Some Metallurgical Aspects of the Dynamic Expansion of Shells, in Shock Waves and High-Strain Rate Phenomena in Metals," ed. M.A. Meyers and L.E. Murr, Plenum Press, New York, 113 (1981).